BIOCHEMISTRY
including biophysical chemistry & molecular biology

Article

pubs.acs.org/biochemistry

Spectroscopic and Calorimetric Studies on the Binding of an Indoloquinoline Drug to Parallel and Antiparallel DNA Triplexes

Fanny Riechert-Krause, Karolin Autenrieth, Andrea Eick, and Klaus Weisz*

Institute of Biochemistry, Ernst-Moritz-Arndt University Greifswald, Felix-Hausdorff-Strasse 4, D-17487 Greifswald, Germany

Supporting Information

ABSTRACT: 11-Phenyl-substituted indoloquinolines have been found to exhibit significant antiproliferative potency in cancer cells but to show only moderate affinity toward genomic double-helical DNA. In this study, parallel as well as antiparallel triple-helical DNA targets are employed to evaluate the triplex binding of these ligands. UV melting experiments with parallel triplexes indicate considerable interactions with the drug and a strong preference for TAT-rich triplexes in line with an increasing number of potential intercalation sites of similar binding strength between two TAT base triads. Via substitution of a singly charged aminoethylamine side chain by a longer and doubly charged bis-(aminopropyl)amine substituent at the ligand, binding affinities increase and also start to exhibit long-range effects as indicated by a strong correlation between the binding affinity and the overall length of the TAT tract within the triplex stem. Compared to parallel triplexes, an antiparallel triplex with a GT-containing third strand constitutes a preferred target for the indoloquinoline drug. On the basis of pH-dependent titration experiments and corroborated by a Job analysis of continuous variation, binding of the drug to the GT triplex not only is strongly enhanced when the solution pH is lowered from 7 to 5 but also reveals a pH-dependent stoichiometry upon formation of the complex. Calorimetric data demonstrate that stronger binding of a protonated drug at acidic pH is associated with a more exothermic binding process. However, at pH 7 and 5, binding is enthalpically driven with additional favorable entropic contributions.

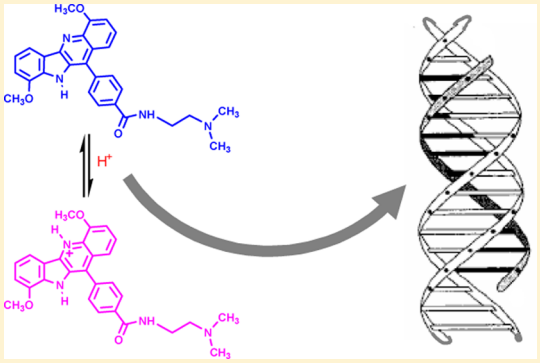

The indoloquinoline ring system constitutes an interesting molecular scaffold for the design of new drugs because of the broad spectrum of biological activities exhibited by many of its derivatives.[1] Naturally occurring indoloquinoline alkaloids are relatively rare and found almost exclusively in *Cryptolepis sanguinolenta*, a climbing shrub indigenous to West Africa. Extracts of the plant have traditionally been used in folk medicine for the treatment of fever from malaria but also for various other disorders. A major constituent of the extracts was characterized as 5-methyl-5*H*-indolo[3,2-*b*]quinoline, commonly known as cryptolepine (Figure 1). Other minor alkaloids isolated include the unsubstituted indolo[3,2-*b*]quinoline or quindoline as well as indoloquinoline regioisomers such as 5-methyl-5*H*-indolo[2,3-*b*]quinoline termed neocryptolepine and 5-methyl-5*H*-indolo[3,2-*c*]quinoline also named isocryptolepine. After the recognition of the wide spectrum of pharmacological properties of cryptolepine and its natural isomers that include antibacterial, antifungal, antiprotozoal, and antitumoral activities, a large number of synthetic indoloquinoline derivatives have been prepared in the recent past and evaluated for their potential biomedical and pharmaceutical value. Thus, cryptolepine derivatives were synthesized and tested for their cytotoxic, antiplasmodial, and antitrypanosomal activities.[2−4] Likewise, a large number of neocryptolepine and isocryptolepine analogues with various substituents and ring substitution patterns have been prepared and evaluated in terms of their cytotoxic effects.[5−7]

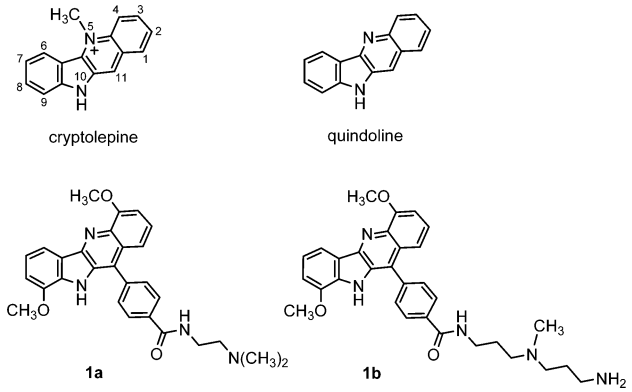

Figure 1. Structure of cryptolepine, quindoline, and analogues **1a** and **1b**.

Whereas the major cellular target and the detailed mechanism of action for the various pharmacological effects of most indoloquinoline drugs remain vague, several binding studies have established that these compounds can intercalate into the DNA double helix with a preference for GC-rich

Received: October 9, 2012
Revised: December 9, 2012
Published: December 12, 2012

dx.doi.org/10.1021/bi301381h | *Biochemistry* 2013, 52, 41−52

sequences, leading to inhibition of DNA synthesis and to the stabilization of topoisomerase II−DNA covalent complexes.[8] For cryptolepine, a crystal structure was reported showing its preferred intercalation between nonalternating CC sites.[9] Subsequent studies have also demonstrated the binding of cryptolepine to triple-helical DNA structures with a preference of triplexes over duplexes.[10] Several quindoline derivatives have also been developed as potential G-quadruplex binding ligands and found to stabilize G-quadruplexes with inhibitory effects on telomerase activity.[11,12]

We have recently reported on the antiproliferative activity of a 4,9-dimethoxy-11-phenyl-substituted quindoline derivative **1a** that has been tethered at the unfused phenyl substituent through formation of an amide bond to a dimethylaminoethyl side chain (Figure 1). The indoloquinoline analogue **1a** showed significant antiproliferative potency in six human cancer cell lines with IC_{50} values in the low micromolar range.[13] On the other hand, binding studies suggested only weak to moderate interactions with double-stranded oligonucleotides. The cytotoxicity and extent of duplex binding of another derivative with the two methoxy substituents at positions C-4 and C-9 substituted for two methyl groups were slightly reduced but suggested no significant impact of the methoxy-to-methyl exchange on the biological activity or DNA binding affinity. In an attempt to improve duplex recognition by third-strand oligonucleotides for antigene applications in molecular biology,[14] therapeutics,[15] or diagnostics,[16] the same indoloquinoline structures were also tethered to triplex-forming oligonucleotides (TFOs) through a simple alkyl linker.[17,18] Detailed thermodynamic and structural studies of DNA triplex formation with a target duplex demonstrated a significant enhancement of triplex formation by the indoloquinoline−TFO conjugates. When tethered to the 5′-terminus of the TFO, the phenyl-substituted indoloquinoline (PIQ) intercalated at the 5′-triplex−duplex junction with the unfused phenyl ring located in the major groove and rotated out of the indoloquinoline plane as revealed by nuclear magnetic resonance spectroscopic analysis.[19] These and other investigations suggest that the unfused 11-phenyl substituent considerably contributes to the binding characteristics of this type of indoloquinolines.

On the basis of the potential of DNA triplexes to serve as powerful tools in various biotechnological and medicinal applications, great effort went into searching for high-affinity ligands with a high triplex selectivity.[20−22] In light of the stabilizing effect on DNA triplexes found for the PIQ analogues when they are conjugated with a TFO, we examined the binding of free PIQ derivatives **1a** and **1b** (Figure 1) to triple-helical oligonucleotides. Both PIQ ligands carry methoxy substituents at ring positions 4 and 9 but differ in their side chain attached to the unfused phenyl ring of the PIQ structure. With its two amino groups, compound **1b** not only has an elongated aminoalkyl chain but also carries an additional positive charge at neutral and acidic pH. Basic amino side chains are expected to have a significant impact on DNA binding, e.g., through electrostatic interactions with the polyanionic sugar−phosphate backbones, but have also been identified as being important contributors to the biological activity of indoloquinoline drugs.[5,6,23] Binding parameters are obtained through a combination of isothermal titration calorimetry, UV melting, fluorescence, and circular dichroism experiments. Employing parallel as well as antiparallel triplex constructs as drug targets, we can evaluate information about the sequence selectivity as well as the pH dependence of drug binding in more detail to provide a more comprehensive understanding of the drug interactions.

MATERIALS AND METHODS

Materials. DNA oligonucleotides were purchased from TIB MOLBIOL (Berlin, Germany). Concentrations of the DNA stock solutions were determined spectrophotometrically from absorbances of single-stranded oligonucleotides using molar extinction coefficients at 260 nm derived from a nearest-neighbor model. Indoloquinoline derivative **1a** was prepared according to previously published procedures.[13,24] Derivative **1b** was synthesized with small modifications in analogy to **1a** (see the Supporting Information). Both indoloquinolines were initially dissolved in small volumes of dimethyl sulfoxide (DMSO) and the concentrated solutions used for the preparation of the final samples. Unless otherwise stated, samples for the parallel triplexes were prepared in 20 mM sodium cacodylate and 100 mM NaCl (pH 6), whereas for the antiparallel triplex, a modified buffer with 20 mM sodium cacodylate and 50 mM $MgCl_2$ adjusted to pH 5, 6, or 7 was used.

UV Melting Experiments. All UV measurements were performed in triplicate using a Cary 100 UV−vis spectrophotometer (Varian, Darmstadt, Germany) with 1 cm path length quartz cells. Absorbances at 260 nm (parallel triplexes) or 280 nm (antiparallel triplex) were recorded in the temperature range of 10−90 °C with one data point per degree Celsius. To prevent the condensation of water on the cuvettes at lower temperatures (<25 °C), the sample chamber was constantly flushed with nitrogen gas. Following an initial annealing step, melting experiments included a first heating ramp (0.5 °C/min), followed by one cooling ramp (0.5 °C/min) and a second heating ramp (0.5 °C/min). The T_m value was taken as the midpoint of the melting transition as determined by the maximum of the first-derivative plot of the second heating curve (Origin 7). For measurements of the drug/DNA mixtures, ligand dissolved in DMSO was added to the DNA solution (total DMSO level of <2%). The same amount of DMSO that was present for the drug/DNA mixtures was added to the free DNA sample without drug.

Fluorescence Spectroscopy. Fluorescence data were recorded at 20 °C with a Jasco (Tokyo, Japan) FP-6500 spectrofluorometer equipped with a Peltier element and a magnetic stirrer. Aliquots of dissolved oligonucleotide were titrated into a 1 cm cuvette with the drug solution (1.5 μM). For titrations with the triplex, the ligand was used either in the absence or in the presence of excess ssDNA (2:1 ssDNA:ligand molar ratio). Both the pure oligonucleotide and the DNA/drug mixture contained an equal percentage of DMSO (<0.2%). Blank corrections were performed through injections of the DNA solution into drug-free buffer. The emission spectra were acquired in the range of 360−650 nm with the excitation wavelength set to 350 nm for the indoloquinoline and excitation and emission bandwidths of 5 nm each. Fluorescence was recorded with a scanning speed of 50 nm/min, a response time of 1 s, and the sensitivity of the photomultiplier set to high or medium. Blank- and volume-corrected emission intensities at 470 nm were normalized and used for the construction of binding isotherms, which were fit to a simple model based on equivalent and independent binding sites.[25,26]

Fluorescence Intercalator Displacement Experiments. Fluorescence intercalator displacement studies of the DNA

dx.doi.org/10.1021/bi301381h | *Biochemistry* 2013, 52, 41−52

Table 1. Oligonucleotide Sequences Used in the Binding Studies

name	sequence	name	sequence
T32	CTTCTTCTT-3' T_4 5'-GAAGAAGAACGC CTTCTTCTTGCG T_4	**T27**	CTTTTTTTC-3' T_4 5'-GAAAAAAAGCGC CTTTTTTTCGCG T_4
T33	CTTTCTTTC-3' T_4 5'-GAAAGAAAGCGC CTTTCTTTCGCG T_4	**D27**	5'-GAAAAAAAGCGC 3'-CTTTTTTTCGCG T_4
T34	CTCTTTTCT-3' T_4 5'-GAGAAAAGACGC CTCTTTTCTGCG T_4	**ss18**	5'-GCGTCT(TTC)$_3$GCG-3'
T35	CTCTTTTTC-3' T_4 5'-GAGAAAAAGCGC CTCTTTTTCGCG T_4	**T_{ap}**	3'-GGGGGTTTTGGG -5' 5'-GGGGGAAAAGGG 3'-CCCCCTTTTCCC T_4

triplexes were performed at 20 °C employing thiazole orange (TO). Serial aliquots of a concentrated ligand solution were added to a mixture of triplex and TO in buffer (1.5 μM **T27** with 3.05 μM TO or 2.9 μM $\mathbf{T_{ap}}$ with 4.5 μM TO). Being mostly unaffected by the indoloquinoline absorption, TO excitation (λ_{ex}) and emission (λ_{em}) wavelengths were set to 504 and 534 nm, respectively. The number of accumulations was typically set to 10 with a waiting time of 5 min before the next titration step to allow for sufficient equilibration.

The volume-corrected TO fluorescence intensity was plotted against the concentration of added ligand and the C_{50} value, given by the concentration of ligand that reduces the TO fluorescence by 50% was extracted. Apparent association constants were calculated using the following equation that can be derived on the basis of competitive binding in analogy to enzyme kinetics in the presence of a competitive inhibitor.[27]

$$K_{a(\text{ligand})} = [1 + c_{(\text{TO})}K_{a(\text{TO})}]/C_{50} \quad (1)$$

where $c_{(\text{TO})}$ and $K_{a(\text{TO})}$ are the TO total concentration and the association constant for thiazole orange for the given triplex and solution conditions, respectively. The latter was determined through separate fluorescence titrations of the TO dye with triplex by fitting the TO emission at 534 nm based on a simple single-site binding model.

CD Spectroscopy. CD spectra were recorded with a J-810 spectropolarimeter (Jasco) equipped with a temperature controller at 20 °C in the range of 210−450 nm for the free DNA. For DNA/ligand mixtures containing small amounts of DMSO, spectra were acquired from 230 to 450 nm because of the strong DMSO absorbance below 230 nm. A 1 cm path length quartz cell was used. Spectra of the DNA samples (2 μM triplex) were recorded at a scan rate of 50 nm/min, a bandwidth of 1 nm, and a response time of 2 s and averaged over up to 20 scans as required. All buffer solutions with and without dissolved oligonucleotide or ligand contained an equal percentage of DMSO (0.5%). All spectra were blank-corrected.

CD titrations were performed at 20 °C by adding aliquots of a ligand DMSO stock solution to the triplex solution. A waiting time of 2 min was used for equilibration before the next titration step. After blank and volume corrections, differences in ellipticity with and without added drug ($\Delta\varepsilon = \varepsilon_{obs} - \varepsilon_{DNA}$) at 247 nm (**T27**) or 280 nm ($\mathbf{T_{ap}}$) were used for the construction of binding isotherms that were fit to a model based on equivalent and independent binding sites.[28]

Job Plot. Job plots were performed in triplicate by mixing different volumes of equimolar stock solutions of ligand and triplex DNA to give a final volume of 2 mL with mole fractions of drug ranging from 0.07 to 0.98. Both the pure oligonucleotide and the pure drug solution contained an equal percentage of DMSO (0.05%). Either the ligand fluorescence at 470 nm or the ellipticity at 280 nm was recorded for each sample and blank-corrected by replacing the triplex or ligand solution with buffer, respectively. Measurements were conducted at 20 °C with spectrometer settings as described for the fluorescence and CD spectra. The binding stoichiometry is given by $n = \chi/(1 - \chi)$, with χ being the mole fraction of the ligand at the inflection point.

Isothermal Titration Calorimetry. ITC experiments were performed with a MicroCal VP-ITC instrument (MicroCal, Northampton, MA) and analyzed with Origin. All samples were dissolved in cacodylate buffer at pH 5 or 7 (0.02 M cacodylate and 50 mM $MgCl_2$) containing additional 10% DMSO for improved ligand solubility. Ligand **1a** (215 μM) was titrated to the triplex solution (200 μM) at 20 °C employing a reference power of 8 μcal/s. The smaller first injection volume (3 μL) was omitted for the final analysis. Subsequent titration steps involved injections with 20 μL each and a delay between injections of 10 min.

Blank titrations were conducted by injecting the ligand into buffer under otherwise identical experimental conditions. The blank-corrected binding enthalpy was directly determined by peak integration of the power output following each injection, normalization by the number of moles of added ligand, and averaging over three independent experiments with five to seven titration steps each. The Gibbs free energy of binding ($\Delta G°$) was calculated from the association constant (K_a) according to the relationship

$$\Delta G° = -RT \ln K_a \quad (2)$$

The entropic contribution $T\Delta S°$ was calculated from the free energy of binding and from the binding enthalpy $\Delta H°$ as determined by the ITC measurements according to the standard thermodynamic relationship

$$\Delta G° = \Delta H° - T\Delta S° \quad (3)$$

RESULTS AND DISCUSSION

Oligonucleotides Employed for the Binding Studies. Table 1 summarizes all sequences that were used in the following binding studies. Because the formation of pyrimidine-type triplexes with third-strand cytosines is known to be strongly pH-dependent, the pH of the buffer for these triple helices was generally adjusted to pH 6. Also, stabilities of short

dx.doi.org/10.1021/bi301381h | Biochemistry 2013, 52, 41−52

triplexes strongly benefit from using intramolecularly folded constructs, allowing for reliable binding studies with a wide range of sequences and solution conditions. Finally, a 3 bp duplex overhang in the parallel triplexes facilitates the analysis of thermal denaturation experiments because of their well-separated duplex and triplex melting. The one-letter code **T** is used to denote a triplex structure and is followed by two numbers in the case of the intramolecular pyrimidine triplexes. These represent the number of cytosine bases within the third strand and the maximal number of contiguous T·AT base triplets within the triplex stem, respectively. In addition to the triplexes of the pyrimidine motif, a hairpin duplex **D27** derived from **T27**, an 18mer single-strand **ss18**, and an antiparallel triplex $\mathbf{T_{ap}}$ with a GT-containing third strand were employed for the thermodynamic studies.

UV Melting Studies of Sequence-Dependent Triplex Binding. Initially, binding of the PIQ ligands was evaluated by UV melting experiments with intramolecular triplex constructs **T32**−**T35** and **T27** as well as with hairpin duplex **D27**, constituting the underlying duplex in **T27** and used as a control. From the temperature-dependent UV absorbances of all triplexes, two melting transitions are observed. The low-temperature transition corresponds to the dissociation of the third strand to form a duplex, and the second high-temperature transition is associated with duplex melting (see Figure S1 of the Supporting Information).

UV melting experiments were performed with the triplexes in the absence and presence of a 10-fold excess of ligand over triplex. Any ligand-mediated change in melting temperature $\Delta T_m^{3\rightarrow2}$ of the triplex−duplex transition is a measure of its triplex binding affinity or, more precisely, its relative triplex versus duplex binding. In general, standard deviations in T_m from three independent measurements were <1 °C (for a compilation of all melting temperatures, see Table S1 of the Supporting Information). Figure 2 shows triplex melting

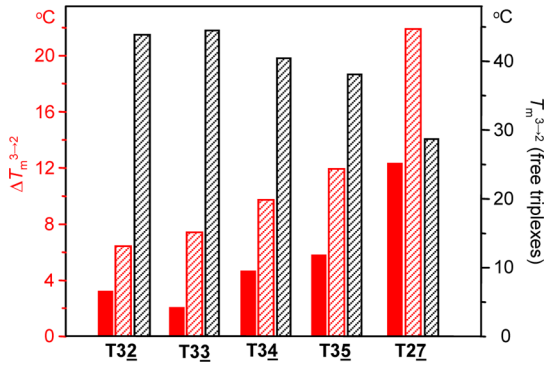

Figure 2. Melting temperatures ($T_m^{3\rightarrow2}$) for the intramolecular pyrimidine triplexes (black) and $\Delta T_m^{3\rightarrow2}$ upon addition of **1a** (solid red) or **1b** (hatched in red). The maximal number of contiguous T·AT triplets in the different triplexes is underlined.

temperatures as well as their changes upon addition of ligand for the various triplexes with their different numbers of contiguous T·AT triplets. Both indoloquinolines **1a** and **1b** stabilize the triplex structures under the given solution conditions. On the other hand, no significant drug-mediated change in any of the high-temperature duplex-to-single strand transitions is observed, and negligible duplex binding of the ligands is also apparent from the melting of hairpin duplex **D27** used as a control (see Table S1 of the Supporting Information).

Thermal stabilization is most pronounced for **T27** with its seven contiguous T·AT base triads. The triplex-to-duplex transition temperature $T_m^{3\rightarrow2}$ of the latter is considerably increased by 12 °C for **1a**, and stabilization is even more pronounced for **1b** ($\Delta T_m^{3\rightarrow2}$ = 22 °C). For the other triplexes having shorter T·AT tracts, drug-induced thermal stabilization is weakened. Thus, the increase in the $T_m^{3\rightarrow2}$ of **T32** with three pairs of two contiguous T·AT triplets amounts to only 3 and 6 °C in the presence of **1a** and **1b**, respectively. Interestingly, thermal stabilization by **1b** seems to strongly correlate with the maximal length of the TAT tracts within the triplexes studied. In contrast, such a correlation is clearly less apparent in the case of **1a**. This points to a more significant impact of the aminoalkyl residue not only on binding affinity but also on the binding selectivity. Obviously, with both amino groups protonated, the two positive charges on the longer bis-amino-functionalized alkyl chain in **1b** are expected to provide stronger electrostatic interactions with the negatively charged phosphodiester backbones in line with the higher level of triplex stabilization of **1b** versus that of **1a**. Also, more favorable interactions with longer T·AT tracts may result from the preferred binding of the aminoalkyl chain in one of the triplex grooves, altered by the particular base sequence. In addition to the minor (Watson−Crick) groove of the triplex, a third strand bound within the major groove of the duplex creates two additional grooves, the small and less accessible Crick−Hoogsteen groove and the larger Watson−Hoogsteen groove. In the case of preferential binding to either the Watson−Crick or Watson−Hoogsteen groove, a stretch of T·AT base triplets will not only influence the pattern of hydrogen bond donor and acceptor sites at the bottom of the grooves but also alter their geometry and electrostatics compared to those of mixed or GC-rich sequences. This sequence discrimination is expected to be strongly attenuated for **1a** because of its shorter and less charged aminoalkyl residue.

Triplex thermal stabilizations by the indoloquinoline ligands provide an easily accessible quantity that is associated with their different extents of binding. This may originate from a different strength of binding at individual binding sites and/or from a different number of binding sites within a triplex. However, changes in melting temperatures cannot be directly translated to relative binding affinities because of additional temperature-dependent effects on ligand binding if melting temperatures differ considerably. With a negative binding enthalpy (vide infra), ligand affinity as measured by the shift in melting temperature will tend to decrease with an increase in stability, i.e., melting temperature of the triplex. Under our solution conditions, melting temperatures of the free triplexes increase in the following order: $T_m^{3\rightarrow2}$(**T27**) < $T_m^{3\rightarrow2}$(**T35**) < $T_m^{3\rightarrow2}$(**T34**) < $T_m^{3\rightarrow2}$(**T32**) ≤ $T_m^{3\rightarrow2}$(**T33**). Disregarding triplex **T27** with a denaturation temperature lower by ≥10 °C compared to those of the other constructs, we found melting temperatures differ by only ≤6 °C and effects of temperature on binding can mostly be neglected in ligand-mediated triplex stabilization. However, they may contribute to the considerable stabilization observed with both indoloquinoline derivatives for **T27**.

In general, triplex-selective intercalators were found to mostly favor T·AT-rich over C^+·GC-rich parallel triplexes, and this sequence selectivity of binding can be attributed to an electrostatic repulsion between the positively charged C^+·GC base triplets and a cationic ligand. As for the triplex itself, C^+·GC triplets are known to confer more stability to triplexes

dx.doi.org/10.1021/bi301381h | *Biochemistry* 2013, 52, 41−52

compared to T·AT triplets if acidic conditions allow for third-strand cytosine protonation. However, they also lead to unfavorable charge−charge repulsion if positioned at neighboring sites.[29,30] As a result, the most stable triplexes carry alternating C^+·GC and T·AT triplets. Similarly, the most stable intercalation complexes were suggested to form when a cationic ligand stacks between uncharged T·AT base triads to give a motif of alternating charged and noncharged units. Consequently, triplexes with alternating C^+·GC and T·AT triplets may hardly be stabilized by cationic ligands because of an associated interruption of this motif upon ligand intercalation.[31]

Adopting the concept of triplex stabilization by charged ligands as mentioned above, the triplex-bound indoloquinoline drugs, expected to be partially protonated at the endocyclic quinoline nitrogen at pH 6,[18] may intercalate only between two T·AT base triads. In addition, the triplex−duplex junction has been found to constitute a strong binding site for the indoloquinoline drugs especially when bordered by a terminal T·AT triplet.[19] Correspondingly, there are six potential high-affinity binding sites in **T27** but only four in triplexes **T32**−**T35**. Minor differences in stabilization by **1a** among the latter triplexes and a much larger enhancement of triplex stability for **T27** point to the overall number of binding sites within the triplexes being the major determinant of sequence-selective stabilization, and no further discrimination of low- and high-affinity binding sites has to be invoked. This contrasts with the triplex stabilization by indoloquinoline **1b**, which also seems to depend on the overall length of the T·AT tract, suggesting some long-range effects exerted by a longer groove-binding aminoalkyl substituent.

Fluorescence Measurements. To mostly address specific binding of the indoloquinoline structure and to limit the largely unspecific polyelectrolyte contribution to the binding free energy, we focused on indoloquinoline derivative **1a** with its less charged side chain for additional thermodynamic studies. In the following, various titration experiments were performed to obtain quantitative binding parameters with triplexes **T27** and **T33**. Initially, the fluorescence emission spectrum of the indoloquinoline drug was recorded upon its titration with triplex DNA. However, nongradual fluorescence changes with a significant hypsochromic shift at the start of titration are not compatible with a simple two-state model and rather indicate the presence of various spectrally distinct species that may also include ligand dimers or even higher-order aggregates (see Figure S2 of the Supporting Information). No attempt was made to fit the binding isotherms with multiple sets of binding parameters. In this case, such an approach will yield only ill-defined values because of convergence problems with too many free-floating parameters.

The fluorescence of the indoloquinolines is very sensitive to their local environment, and even weak binding of the indoloquinolines in the presence of single-stranded DNA triggers significant changes in ligand fluorescence with an up to 20-fold fluorescence enhancement observed for **1a** (see Figure S3 of the Supporting Information). In an attempt to separate specific triplex binding from processes associated with weak and less specific electrostatic interactions with the polyanionic DNA backbone, a single-stranded oligonucleotide was added to the ligand prior to its titration with the DNA triplex target. In this case, a direct transfer of ligand associated with ssDNA to a specific binding site in the triple-helical complex is expected to simplify titration data for subsequent analysis. Indeed, titrating a mixture of **1a** and **ss18** in a 1:2 molar ratio with triplex **T27** yields a continuous change in the indoloquinoline fluorescence in line with a simple two-state equilibrium (Figure 3). Most

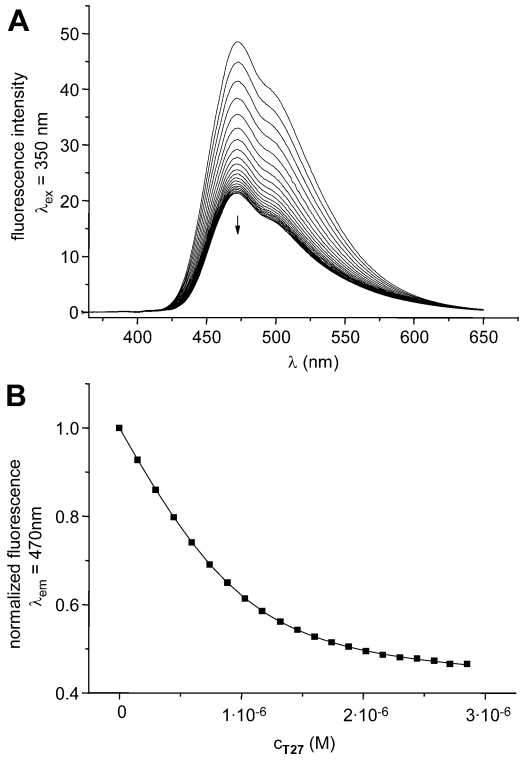

Figure 3. (A) Fluorescence emission spectra upon titration of ligand **1a** (1.5 μM) in the presence of **ss18** (1:2 molar ratio) with triplex **T27** at 20 °C. The arrow follows spectra with an increasing triplex concentration. (B) Binding isotherm from the normalized fluorescence at 470 nm and least-squares fit.

notably, together with a small hypsochromic shift for the emission maximum of ∼3 nm, a quenching of the fluorescence by ∼56% is observed upon addition of the triplex, and thus, this result contrasts with the result of titration of the ligand solution without ssDNA. It should be mentioned that triplex binding of a corresponding indoloquinoline ligand conjugated to a TFO showed a decrease in fluorescence upon formation of the triplex with the addition of a duplex target, and this fluorescence quenching could be attributed to ligand intercalation.[18] Therefore, the fluorescence data obtained under these conditions likely reflect intercalation of PIQ between base triads of the triplex.

The titration data in the presence of excess single strand were amenable to a separate determination of binding stoichiometries and association constants (K_a), characterizing binding to true binding sites in the triple-helical DNA construct. However, they must be regarded as lower limits because additional less specific interactions in the presence of nucleic acids have been partially eliminated by the experimental setup. In line with the UV melting data on the sequence-dependent thermal stabilization, association constants and stoichiometries for binding of **1a** to triplexes **T33** and **T27** suggest binding sites of about equal strength but the presence of more binding sites in the latter triplex (see Table 2). Thus, fitting of the experimental data gives K_a values of 3−4 × 10^6 M^{-1} but suggest a 2:1 stoichiometry for **1a** in the case of the **T27** triplex but a binding ratio of only 1:1 when binding triplex **T33**.

dx.doi.org/10.1021/bi301381h | *Biochemistry* 2013, 52, 41−52

Table 2. Association Constants (K_a) and Ligand-to-Triplex Stoichiometries (n) for the Binding of 1a to Triplex DNA As Determined by Various Spectroscopic Methods

	K_a ($\times 10^6$ M^{-1})			n		
T33	3.9 ± 0.7[a]			0.9[a]	1.3 ± 0.1[b]	
T27	3.1 ± 0.1[a]	2.6 ± 0.6[c]	4.6 ± 2.4[d]	1.5[a]	1.8 ± 0.1[b]	2.1[d]

[a]Determined from fluorescence titrations in the presence of ssDNA **ss18** (2-fold excess over ligand). [b]Determined from Job analysis of ligand fluorescence. [c]Determined from thiazole orange displacement studies based on strictly competitive binding. [d]Determined from CD titrations.

To further verify stoichiometries as extracted from the fitting of the binding isotherms, a Job analysis based on the ligand fluorescence was used as an independent method for the determination of binding stoichiometries. Job plots constructed with mixtures of different **1a**:triplex molar ratios but with a fixed total concentration are shown in Figure 4. Linear least-squares fitting gives ligand mole fractions (χ) of 0.65 and 0.58 at the intersection point in the case of **T27** and **T33**, respectively. Corresponding stoichiometries of 1.8 and 1.3 again point to the presence of more binding sites in triplex **T27** under these conditions and suggest a 2:1 molar ratio for the **1a**–**T27** complex (Table 2).

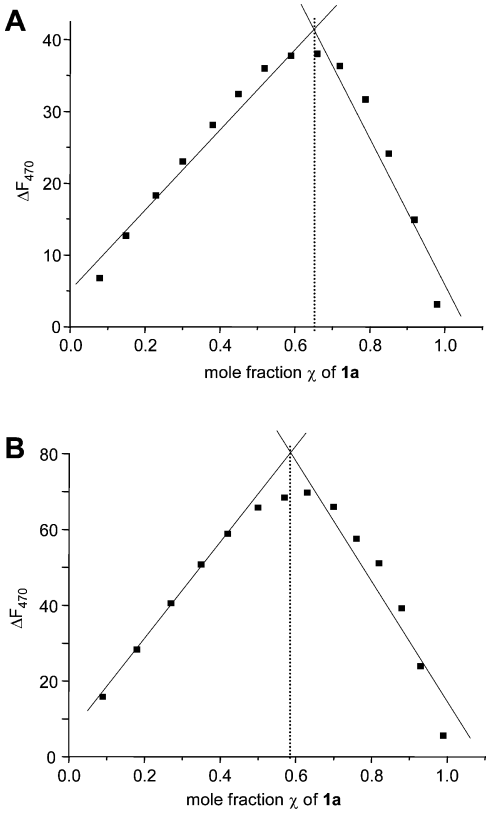

Figure 4. Job plots constructed by measuring the fluorescence of **1a** in mixtures of **1a** and **T27** (A) or **T33** (B) at variable molar ratios but with a fixed total concentration. T = 20 °C, and λ_{ex} = 350 nm.

In trying to minimize problems associated with the more complex fluorescence behavior of the ligands, we employed additional fluorescence intercalator displacement (FID) studies for an assessment of binding toward triplex **T27**.[32,33] The use of thiazole orange (TO) as a fluorescent probe in the displacement assays on triplexes benefits from its high affinity for triple-helical DNA and its large fluorescence enhancement upon intercalation into the nucleic acid.[34] Employing the FID method, relative binding affinities for a family of related ligands can be conveniently evaluated from a comparison of the corresponding ligand concentrations (C_{50}) required to reduce the TO fluorescence through its displacement by 50%.[35,36] On the other hand, knowing the association constant of TO under the given conditions also allows for a more quantitative assessment of ligand binding. Thus, ligand association constants can be directly deduced from C_{50} values provided that there is a strictly competitive binding between TO and the ligand under examination (see Materials and Methods).

Figure 5 shows the course of TO fluorescence upon titration of **1a** into a solution of TO and triplex **T27**. The TO displacement by the indoloquinoline ligand results in a gradual quenching of TO fluorescence. With a negligible fluorescence of free TO, the amount of displaced intercalator directly follows the observed decrease in TO fluorescence and yields a C_{50} of 11 μM as a measure of **1a** binding affinity (Figure 5). Given the association constant of TO for triplex **T27** that has been determined in separate fluorescence titration experiments under the same solution conditions [$K_{a(TO)}$ = (9.6 ± 1.8) × 10^6 M^{-1} at pH 6 and 20 °C], a triplex binding constant K_a of 2.6 × 10^6 M^{-1} can be calculated assuming strictly competitive binding (Table 2). Corresponding TO displacement titrations with **1b** yield a C_{50} value of 5 μM (not shown). This translates to a K_a of 5.5 × 10^6 M^{-1} and confirms the higher triplex affinity of the more positively charged **1b** in line with the UV melting experiments.

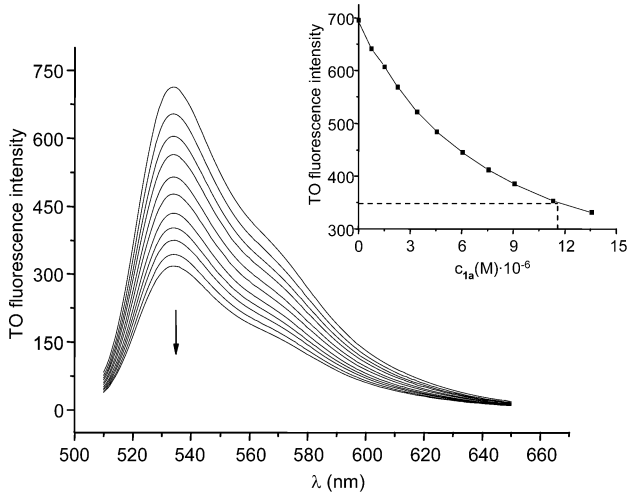

Figure 5. Displacement titration showing a decrease in the fluorescence of thiazole orange (λ_{ex} = 504 nm) in a complex with **T27** upon addition of **1a**. The inset shows the TO fluorescence intensity at a λ_{em} of 534 nm plotted vs added ligand; the dotted line indicates the concentration of **1a** at 50% TO fluorescence quenching. T = 20 °C.

Circular Dichroism Experiments. Association constants derived from direct titrations of the ligand with triplex and fluorescence displacement experiments are in surprisingly good

dx.doi.org/10.1021/bi301381h | Biochemistry 2013, 52, 41–52

agreement given the shortcomings of the experimental setup and data analysis (vide supra). Thus, eliminating some binding free energy by adding ssDNA before titration or assuming equal triplex binding sites for TO and the indoloquinoline ligand will likely introduce some error into the extracted parameters. It must be noted, however, that binding constants will tend to be underestimated in both cases. To further validate the extracted binding constants and to assess possible uncertainties in K_a, we performed additional circular dichroism (CD) experiments. By titrating triplex DNA with the ligand, CD spectral changes below 300 nm can mostly be attributed to structural rearrangements of the DNA upon ligand binding irrespective of other ligand species free in solution or only weakly bound. Also, at the beginning of the titration, the triplex will be in large excess over the ligand in contrast to the reversed fluorescence titrations described above, and this may influence corresponding binding isotherms in cases of different binding sites with noticeably different binding affinities.

In addition to a negative band at 250 nm and a positive band at 280 nm, the CD spectrum of free **T27** exhibits a negative CD amplitude in the range of 210−220 nm characteristic of triplex formation (Figure 6A). On the other hand, free indoloquinoline **1a** shows no CD effect over the entire wavelength region as expected from an achiral molecule. Upon addition of **1a** to the triplex, the CD spectrum of the triplex changes as a result of ligand binding. Thus, the negative band at 250 nm shifts to longer wavelengths, and its amplitude decreases. In contrast, only rather small changes in wavelength and intensity are observed for the long-wavelength maximum at 280 nm. An assessment of the high-amplitude negative band at 210 nm was not possible because of the strong absorbance of small amounts of DMSO present in the mixture. Centered at the long-wavelength absorbance maximum of **1a** at ∼350 nm, a weak but noticeable induced CD (ICD) appears as a result of **1a** bound in an asymmetric environment and again points to an intercalative mode of binding (see the inset of Figure 6A).

For the construction of binding isotherms, the triplex was titrated with **1a** up to a final molar ratio of 1:5 and changes in ellipticity ($\Delta\varepsilon$) at 247 nm were plotted versus the concentration of **1a** (Figure 6B). A nonlinear fit of the data yields an association constant (K_a) of 4.6 × 10^6 M^{-1} and a stoichiometry of 2.1 (Table 2). As is apparent from Figure 6B, changes in ellipticity during titration are rather small, resulting in a relatively wide variability of the experimental data with associated larger uncertainties in the fitted parameters. Nevertheless, the extracted stoichiometry confirms the presence of two binding sites occupied by **1a** in triplex **T27** with an affinity close to what has been determined by fluorescence experiments, lending additional confidence to the binding parameters as summarized in Table 2. The affinity as determined here for the PIQ drug seems to be superior to the triplex binding of the related cryptolepine alkaloid. Thus, association constants in the range of 10^5−10^6 M^{-1} for the binding of cryptolepine to a corresponding pyrimidine-type triple-helical oligonucleotide have previously been reported on the basis of mass spectral peak intensities.[10]

pH-Dependent Binding Studies of Antiparallel Triplexes. The bimolecular T_{ap} construct was designed to allow only the formation of a triplex with an antiparallel orientation of the GT-containing third strand relative to the purine strand of the hairpin target. A modified buffer with 20 mM sodium cacodylate and 50 mM $MgCl_2$ was found to ensure sufficient triplex stability and was used for subsequent measurements. CD

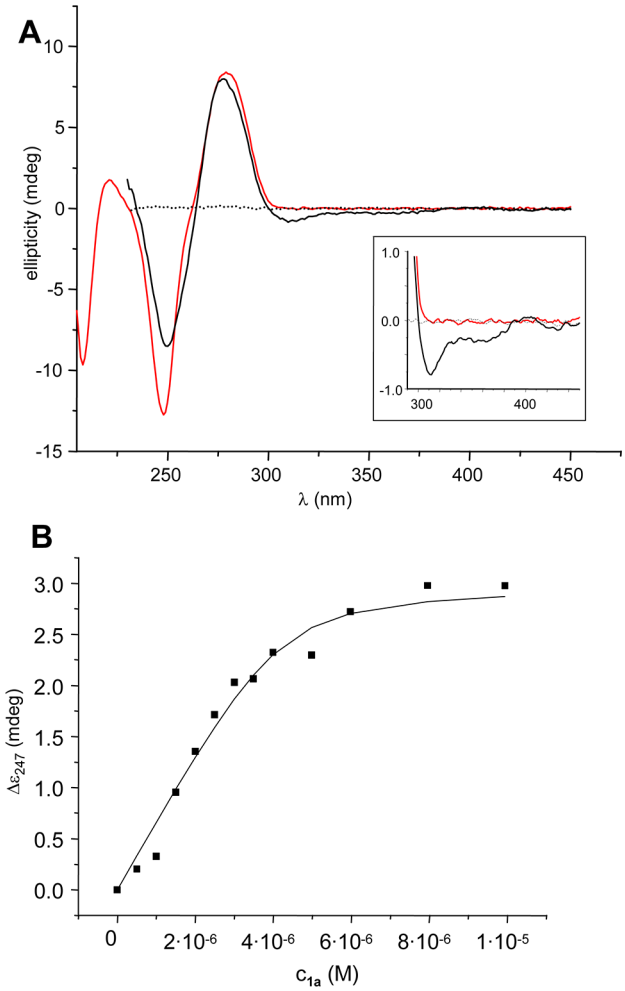

Figure 6. (A) CD spectra at 20 °C of free **1a** (10 μM, dotted), free **T27** (2 μM, red), and a mixture of **1a** with **T27** (5:1 molar ratio, black). The inset shows an expanded view over the region of **1a** absorbance with induced CD effects. (B) Changes in ellipticity at 247 nm upon titration of **T27** (2 μM) with **1a**. The curve represents the nonlinear fit of the data to a binding isotherm.

spectra acquired at 20 °C under these buffer conditions confirm the formation of a stable triplex structure that is insensitive to pH within the range of 5−7 (see Figure S4 of the Supporting Information). Likewise, UV melting experiments with T_{ap} show two pH-independent transitions at ∼41 and ∼80 °C that can be attributed to the dissociation of the triplex third strand and the melting of the hairpin duplex (see also Table 3).

Initially, binding of **1a** to the antiparallel triplex was evaluated by UV melting of T_{ap} in the presence of excess ligand. Whereas no noticeable change in the duplex melting temperature upon addition of **1a** is observed, triplex thermal stability significantly increases as indicated by a shift of the triplex melting temperature ($T_m^{3\to2}$) from 41 to 59 °C at pH 6. This increase of 18 °C ($\Delta T_m^{3\to2}$) upon binding **1a** points to an even larger stabilization and thus affinity for the GT triplex when compared to the **T27** pyrimidine-type triplex. The latter exhibits a $\Delta T_m^{3\to2}$ of 12 °C in the presence of **1a** at the same pH, albeit under different salt conditions (see Table 3).

Triplex affinities of PIQ ligands seem to strongly depend on pH.[18,19] In fact, a pK_a value of 4.5 was determined for the N5 ring protonation of free indoloquinoline **1a**, excluding a significant population of protonated free drug at pH ≥6.

dx.doi.org/10.1021/bi301381h | *Biochemistry* 2013, 52, 41−52

Table 3. UV Melting Temperatures as a Function of pH for T27 and T_{ap} Triplexes with and without 1a[a]

	$T_m^{3\to2}$ (°C)	$T_m^{2\to1}$ (°C)	$\Delta T_m^{3\to2}$ (°C)	$\Delta T_m^{2\to1}$ (°C)
T_{ap}, pH 5.0	40.8 ± 1.0	79.1 ± 1.0		
T_{ap} with **1a**, pH 5.0	65.4 ± 1.0	79.2 ± 1.0	24.6 ± 1.4	0.1 ± 1.4
T27, pH 5.5	38.1 ± 0.6	74.1 ± 0.8		
T27 with **1a**, pH 5.5	53.3 ± 0.7	73.5 ± 0.7	15.2 ± 0.9	0.6 ± 1.1
T_{ap}, pH 5.5	39.7 ± 0.9	80.9 ± 0.1		
T_{ap} with **1a**, pH 5.5	61.1 ± 0.9	82.2 ± 0.5	21.4 ± 1.2	1.3 ± 0.5
T27, pH 6.0	28.7 ± 0.2	74.0 ± 0.6		
T27 with **1a**, pH 6.0	41.0 ± 0.3	74.3 ± 0.7	12.3 ± 0.4	0.3 ± 0.9
T_{ap}, pH 6.0	41.0 ± 1.1	80.9 ± 0.7	–	–
T_{ap} with **1a**, pH 6.0	58.8 ± 1.6	81.7 ± 1.3	17.8 ± 1.9	0.8 ± 1.5
T27, pH 7.0	12.6 ± 0.5	75.0 ± 0.7		
T27 with **1a**, pH 7.0	22.9 ± 0.5	75.2 ± 0.6	10.3 ± 0.7	0.2 ± 0.9
T_{ap}, pH 7.0	40.7 ± 0.4	80.9 ± 0.2		
T_{ap} with **1a**, pH 7.0	55.0 ± 0.5	80.8 ± 0.4	14.3 ± 0.6	−0.1 ± 0.4

[a]Averaged T_m values with standard deviations from three independent measurements for a mixture of triplex (1 μM) and ligand (10 μM). Because of the partial overlap of triplex and duplex transitions at pH 5.0 in the presence of ligand, the ΔT_m of **T27** was measured at only pH ≥5.5.

However, when the drug is bound to a DNA triplex, apparent pK_a values as measured with an all-TAT triplex target increase by approximately two pK_a units to give a pK_a^{app} of ~6.7 (see Table S2 of the Supporting Information). This suggests that protonation equilibria may have a large impact on ligand binding under the experimental conditions used here. Correspondingly, the triplex thermal stabilization after the addition of **1a** increases with a decreasing pH for both parallel and antiparallel triplexes (Table 3). In the presence of ligand, $\Delta T_m^{3\to2}$ increases from 10 to 15 °C for **T27** and from 14 to 21 °C for T_{ap} when the pH is lowered from 7 to 5.5. A remarkable stabilization for T_{ap} by ~25 °C is even observed in a more acidic solution at pH 5. It should be kept in mind, however, that the stability of a parallel triple helix itself exhibits a strong pH dependence because protonation of third-strand cytosines is required to form two stable Hoogsteen hydrogen bonds within a C^+·GC base triad. This is clearly evident when following the triplex melting temperature of free **T27** with pH (Table 3). Thus, $T_m^{3\to2}$ varies by ~25 °C within a pH range of 5.5−7, adding non-negligible temperature-dependent effects on binding to the observed ligand-induced thermal stabilizations. Because the latter effects cannot be strictly separated from effects arising from protonation equilibria on the indoloquinoline, a more detailed assessment of the pH-dependent ligand affinity is severely hampered. On the other hand, antiparallel triplex T_{ap} shows no pH dependence within the pH range examined and pH-dependent effects on the thermal stability of T_{ap} complexes can be directly interpreted in terms of relative drug binding affinities.

Fluorescence Intercalator Displacement (FID). To scrutinize the pH-dependent triplex affinity of the ligand, T_{ap} was employed in the following as a triplex target for the PIQ ligand. Initially, fluorescence intercalator displacement studies with thiazole orange as a reporter fluorophore were performed at pH 6 in analogy to the FID assays on the triplex binding to **T27**. A **1a** concentration of 6.6 μM (C_{50}) at 50% TO fluorescence quenching was determined under these conditions and used together with the independently obtained TO association constant for T_{ap} binding to derive a K_a of 6.5 × 10^6 M^{-1} (see Figure S5 and Table S3 of the Supporting Information). As already indicated by the UV melting experiments (Table 3), binding of the indoloquinoline to the antiparallel triplex is characterized by an association constant (K_a) increased by a factor of ~2 when compared to the parallel triplexes (see Table 2).

Being stable in a neutral solution, the T_{ap} triplex was employed for additional FID experiments at pH 7. Because an altered pH is also expected to have an impact on the triplex binding of the TO dye, the TO association constant at pH 7 was again determined in preliminary fluorescence titration experiments and used to derive a corresponding $K_{a(1a)}$ of 1.7 × 10^6 M^{-1} from the **1a** concentration at 50% TO fluorescence (see Figure S5 and Table S3 of the Supporting Information). Remarkably, the PIQ binding shows a 4-fold increase in K_a when the pH is lowered from 7 to 6.

CD Measurements. Adding **1a** in a 3-fold excess to the T_{ap} triplex results in pH-dependent changes of the triplex circular dichroism spectrum. As shown in Figure 7, the DNA negative

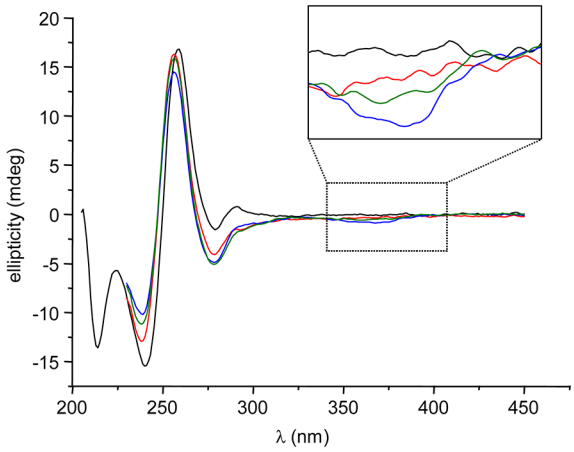

Figure 7. CD spectra of T_{ap} in the presence of **1a** (1:3 molar ratio) at pH 5 (blue), 6 (green), and 7 (red) as well as the sum of individual T_{ap} and **1a** spectra at pH 7 (black). The inset shows an expanded view over the region of **1a** absorbance with induced CD effects. T = 20 °C.

and positive maxima at ~240 and ~260 nm decrease in amplitude, and these effects are clearly enhanced with a decrease in pH. Also, a smaller negative amplitude at 280 nm increases upon drug binding. As for the binding of parallel triplexes, a low-intensity negative ICD band in the **1a** absorption range centered at 360 nm points to intercalation of the ligand between base triads of the antiparallel triplex. Stronger ligand binding with a decrease in pH is again apparent from the ICD amplitude (see Figure 7).

In the following, circular dichroism was used to determine association constants and stoichiometries of **1a** binding to T_{ap}. Upon titration of the triplex with aliquots of a ligand solution, changes in ellipticity at 280 nm were recorded and used for the construction of a corresponding binding isotherm (Figure 8). Fitting the data with a model based on equivalent and independent binding sites points to a 1:1 stoichiometry and

dx.doi.org/10.1021/bi301381h | *Biochemistry* 2013, 52, 41−52

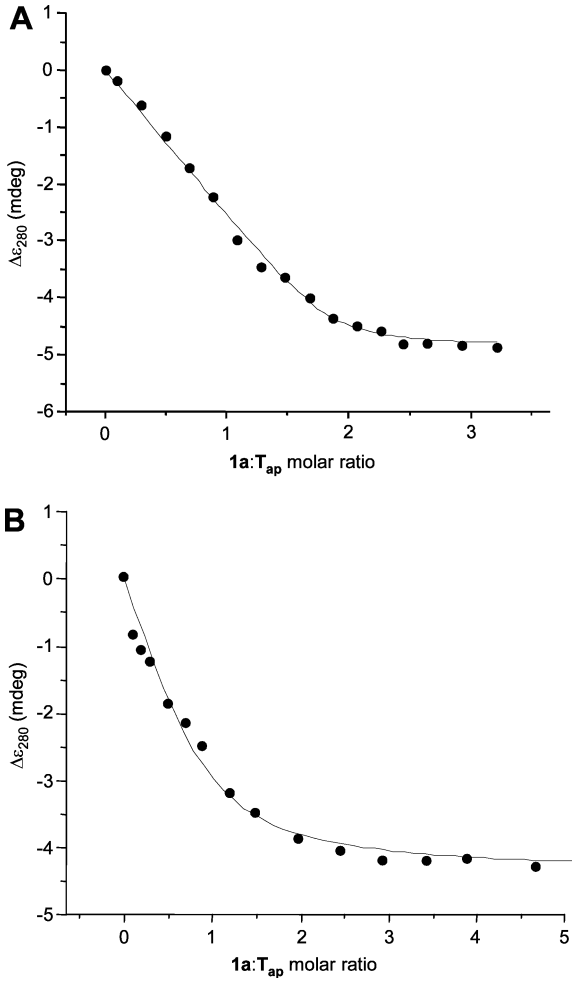

Figure 8. Circular dichroism binding isotherms from the titration of triplex $\mathbf{T}_{ap}$ (3 μM) with **1a** at pH 5 (A) and pH 7 (B). A fit to the data was conducted using a nonlinear least-squares analysis based on equivalent and independent binding sites. T = 20 °C.

yields a K_a of 1.8 × 10^6 M^{-1} at pH 7, in excellent agreement with the thiazole orange displacement studies (vide supra). Another titration in an acidic medium at pH 5 yields a corresponding K_a larger by nearly 1 order of magnitude (Table 4), in line with the pH dependence of triplex affinity as already indicated by the FID assays. Interestingly, the number of binding sites is also altered and indicates a 2:1 stoichiometry at acidic pH.

To independently verify pH-dependent stoichiometries when binding to the antiparallel triplex, Job plots through the method of continuous variation were constructed by recording CD spectral changes at pH 7 and 5. Here, clear inflection points again characterize stoichiometries of 1:1 and 2:1 for pH 7 and 5, respectively, and confirm results from the fitting of the titration data (see Figure S6 of the Supporting Information). Obviously, the number of potential binding sites not only is determined by the DNA target sequence but also is dependent on pH and thus largely on the protonation state of the indoloquinoline drug.

Isothermal Titration Calorimetry. Isothermal titration calorimetry (ITC) allows for the direct determination of the molar binding enthalpy but has only rarely been exploited in the analysis of triplex binding ligands.[37,38] Having already determined reliable association constants by the fitting of titration data based on changes in ellipticity, an extraction of binding enthalpies provides a thermodynamic profile of the binding reaction. Binding enthalpies were directly measured in a model-independent fashion through the excess-site method.[39,40] In this protocol, an excess amount of triplex $\mathbf{T}_{ap}$ is placed inside the sample cell and titrated with small amounts of the indoloquinoline to ensure complete binding of ligand to the triplex following each injection. Under such conditions, the integration of each injection peak corrected for the heat of dilution of **1a** yields the heat released per injection and its normalization per mole of added ligand directly results in the molar binding enthalpy (Figure 9).

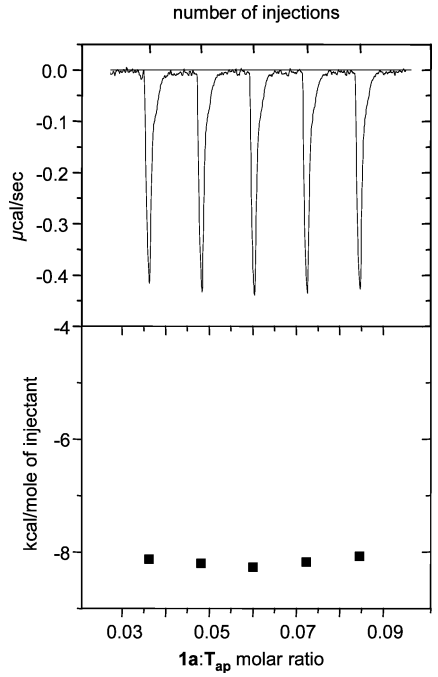

Figure 9. Calorimetric data for the titration of excess $\mathbf{T}_{ap}$ with indoloquinoline **1a** at 20 °C and pH 5 showing exothermic binding. ITC raw data give the power output for five consecutive 20 μL injections of titrant and are presented in the top panel. The bottom panel was obtained after peak integration and shows the molar heat produced per injection as a function of the ligand:triplex molar ratio (■). The initial triplex concentration in the sample cell was 200 μM, and the concentration of ligand titrant was 215 μM.

Table 4. Summary of Thermodynamic Parameters for the Binding of 1a to Triplex $\mathbf{T}_{ap}$ As Determined by Spectroscopic and Calorimetric Methods at 20 °C

	K_a (×10^6 M^{-1})[a]	n^a	n^b	$\Delta G°$ (kcal/mol)[c]	$\Delta H°$ (kcal/mol)[d]	$-T\Delta S°$ (kcal/mol)
pH 5	13 ± 1.0	1.9	2.2	−9.5	−8.3 ± 0.2	−1.2
pH 7	1.8 ± 0.5	1.1	1.0	−8.4	−5.2 ± 0.3	−3.2

[a]Determined from the fitting of CD titration data. [b]Determined from Job analysis based on CD spectral changes. [c]Derived from K_a. [d]Determined from model-free ITC.

dx.doi.org/10.1021/bi301381h | *Biochemistry* 2013, 52, 41−52

Binding enthalpies averaged over three independent titration experiments with five to seven injections each are given for pH 5 and 7 in Table 4. Table 4 also includes standard free energies and entropies that have been calculated using association constants as derived by the CD titration experiments. Thermodynamic parameters of the indoloquinoline binding noticeably differ depending on the pH conditions. The more favorable binding free energy (ΔG°) at acidic pH largely results from a considerably more exothermic binding of a protonated drug that seems to form more and also stronger specific interactions with the triple-helical target. These may involve stacking interactions with base triplets, being altered by the indoloquinoline ring protonation through changes in the permanent indoloquinoline dipole moment as well as in its polarizability. However, on the basis of an increase of approximately 2 pK_a units upon triplex binding, intercalation of the drug is also expected to be linked with protonation in the PIQ ring system over the pH range studied. Consequently, the observed enthalpy as measured by the ITC experiment includes not only the intrinsic heat of drug binding but also additional heat for the protonation processes. Because the extent of binding-linked protonation and thus the heat of ligand protonation will depend on pH, a direct assessment of pH-dependent enthalpies in terms of specific interactions should be treated with caution. There is some entropy−enthalpy compensation, but the less negative ΔH° at pH 7 is only partially compensated by an associated more favorable entropic term. However, binding at both neutral and acidic pH is mostly enthalpy-driven, yet a favorable entropy also contributes to the binding interaction.

An average binding free energy for typical monointercalators has previously been estimated to amount to −7.3 ± 0.8 kcal/mol.[41,42] By comparison, the ΔG° for binding of **1a** to the triplex in an acidic but also in a neutral medium is quite exergonic and thus associated with a high binding affinity when disregarding uncertainties caused by binding-linked protonation as discussed above. On the other hand, the indoloquinoline clearly fits the thermodynamic signature that has been found for a variety of DNA duplex intercalators. Whereas binding of intercalators is expected to be driven by a large and favorable enthalpy, complex formation with groove-binding ligands is often entropically driven and may even be associated with endothermic binding.[41−43]

It is also instructive to compare the thermodynamic signature of triplex binding for the present indoloquinoline with that of an indoloquinoline analogue conjugated through an alkyl linker to a third-strand oligonucleotide.[18] The thermodynamics in the latter case has been determined from the difference in spectroscopically and calorimetrically derived free energies and enthalpies for the duplex binding of an oligonucleotide−ligand conjugate and of a corresponding nonconjugated TFO. The extracted $\Delta\Delta G^\circ$ of only −1.8 kcal/mol at pH 6 can be regarded as being a good measure of exclusive ligand binding effects in the triplex conjugate. Also, the thermodynamic profile with the conjugate indicated a larger contribution from entropy and only slightly exothermic binding in contrast to the case for the free indoloquinoline. The latter observation may be attributed to (i) considerable stacking interactions of the ligand with nucleobases already present within the free TFO conjugate, (ii) the restricted flexibility of the tethered ligand, hampering its geometric rearrangement to optimize interactions after triplex formation, and (iii) significant additional contributions to binding of the positively charged aminoalkyl residue in free **1a** within a triplex groove. Nonetheless, the less favorable free energy of triplex binding for the tethered ligand might seem counterintuitive given the significant thermal stabilizations observed for triplexes formed with such TFO−ligand conjugates.[17,18] However, coupling with third-strand binding and associated cooperativity effects inevitably lead to a much better discrimination of triplex versus duplex for the TFO-conjugated ligand, markedly increasing its effectiveness for triplex thermal stabilizations as, for example, measured by UV melting experiments.

CONCLUSIONS

In contrast with their only weak binding to duplex DNA, 11-phenyl-substituted indolo[3,2-*b*]quinoline derivatives exhibiting significant in vitro anticancer activity bind with high affinity to triple-helical DNA. Triplex binding is strongly dependent on the base sequence of the nucleic acid target as well as on the pH of the medium. Thus, a charged aminoalkyl residue with a propensity to bind within a DNA groove is expected to increase the ligand affinity through additional electrostatic and van der Waals interactions but may also substantially add to the sequence selectivity of the indoloquinoline intercalator by probing the shape and electrostatic potential within the occupied groove. Protonation of the indoloquinoline at pH <7 strongly enhances its ability to bind to parallel as well as antiparallel triplexes through strengthened stacking interactions, contributing to a more favorable enthalpic term for binding; however, drug protonation may also alter the complex stoichiometry, and this often unnoticed impact of pH on the number of drug binding sites may be another major contributor to the ligand-mediated triplex thermal stabilization as generally measured by DNA melting experiments.

With their marked preference for triplex over duplex structures, these indoloquinolines represent triplex binding ligands with excellent triplex selectivities. Although some naturally occurring DNA sequences are thought to represent a source of genetic instability and to regulate the expression of disease-linked genes through the transient formation of triplex structures such as H-DNA,[44] a direct link between the biological activity of the PIQ drugs and their binding to cellular triplexes is difficult to establish and remains elusive to date. In addition to possible applications in therapy, bioanalytical assays for the detection of duplex sequences without their prior denaturation based on a triplex strategy are expected to strongly benefit from high-affinity triplex ligands. With their strong triplex versus duplex discrimination, these PIQ ligands might also be useful for direct detection of DNA triple helices. However, the relatively poor fluorescence signal upon triplex binding will restrict their use for corresponding applications because of an associated low sensitivity of the diagnostic system in the absence of another signal transducer. Therefore, appropriate modifications to enhance the binding-induced PIQ fluorescence are highly desirable. The detailed thermodynamic and spectroscopic analysis provides a basis for the rational drug design of new indoloquinoline derivatives with superior properties in terms of triplex affinity, selectivity, and optical characteristics. Of course, additional structural information will be needed in the future to complement thermodynamic data and to assess binding from both thermodynamic and structural perspectives.

dx.doi.org/10.1021/bi301381h | *Biochemistry* 2013, 52, 41−52

■ ASSOCIATED CONTENT

Supporting Information

Experimental details of the synthesis and spectroscopic characterization of indoloquinoline **1b**, UV melting curves and summary of melting temperatures of parallel triplexes, fluorescence quantum yields and pK_a values for indoloquinoline **1a**, fluorescence titrations of **1a** with triplex **T27** and single-strand **ss18**, CD spectra of antiparallel triplex $\mathbf{T}_{ap}$, and pH-dependent FID experiments and Job plots for the analysis of binding of **1a** to triplex $\mathbf{T}_{ap}$. This material is available free of charge via the Internet at http://pubs.acs.org.

■ AUTHOR INFORMATION

Corresponding Author

*Institute of Biochemistry, Ernst-Moritz-Arndt University Greifswald, Felix-Hausdorff-Str. 4, D-17487 Greifswald, Germany. Telephone: +49 (0)3834 864426. Fax: +49 (0)3834 864427. E-mail: weisz@uni-greifswald.de.

Notes

The authors declare no competing financial interest.

■ ABBREVIATIONS

PIQ, 11-phenyl-10*H*-indolo[3,2-*b*]quinoline; TO, thiazole orange; FID, fluorescence intercalator displacement; CD, circular dichroism; ICD, induced circular dichroism; ITC, isothermal titration calorimetry.

■ REFERENCES

(1) Lavrado, J., Moreira, R., and Paulo, A. (2010) Indoloquinolines as scaffolds for drug discovery. *Curr. Med. Chem. 17*, 2348−2370.

(2) Arzel, E., Rocca, P., Grellier, P., Labaeïd, M., Frappier, F., Guéritte, F., Gaspard, C., Marsais, F., Godard, A., and Quéguiner, G. (2001) New synthesis of benzo-*δ*-carbolines, cryptolepines, and their salts: In vitro cytotoxic, antiplasmodial, and antitrypanosomal activities of *δ*-carbolines, benzo-*δ*-carbolines, and cryptolepines. *J. Med. Chem. 44*, 949−960.

(3) Gopalan, R. C., Emerce, E., Wright, C. W., Karahalil, B., Karakaya, A. E., and Anderson, D. (2011) Effects of the anti-malarial compound cryptolepine and its analogues in human lymphocytes and sperm in the Comet assay. *Toxicol. Lett. 207*, 322−325.

(4) Lavrado, J., Mackey, Z., Hansell, E., McKerrow, J. H., Paulo, A., and Moreira, R. (2012) Antitrypanosomal and cysteine protease inhibitory activities of alkyldiamine cryptolepine derivatives. *Bioorg. Med. Chem. Lett. 22*, 6256−6260.

(5) Luniewski, W., Wietrzyk, J., Godlewska, J., Świtalska, M., Piskozub, M., Peczyńska-Czoch, W., and Kaczmarek, L. (2012) New derivatives of 11-methyl-6-[2-(dimethylamino)ethyl]-6*H*-indolo[2,3-*b*]quinoline as cytotoxic DNA topoisomerase II inhibitors. *Bioorg. Med. Chem. Lett. 22*, 6103−6107.

(6) Wang, L., Świtalska, M., Mei, Z.-W., Lu, W.-J., Takahara, Y., Feng, X.-W., El-Sayed, I. E.-T., Wietrzyk, J., and Inokuchi, T. (2012) Synthesis and in vitro antiproliferative activity of new 11-amino-alkylamino-substituted 5*H*- and 6*H*-indolo[2,3-*b*]quinolines; structure-activity relationships of neocryptolepines and 6-methyl congeners. *Bioorg. Med. Chem. 20*, 4820−4829.

(7) Lu, C.-M., Chen, Y.-L., Chen, H.-L., Chen, C.-A., Lu, P.-J., Yang, C.-N., and Tzeng, C.-C. (2010) Synthesis and antiproliferative evaluation of certain indolo[3,2-*c*]quinoline derivatives. *Bioorg. Med. Chem. 18*, 1948−1957.

(8) Bonjean, K., De Pauw-Gillet, M. C., Defresne, M. P., Colson, P., Houssier, C., Dassonneville, L., Bailly, C., Greimers, R., Wright, C., Quetin-Leclercq, J., Tits, M., and Angenot, L. (1998) The DNA intercalating alkaloid cryptolepine interferes with topoisomerase II and inhibits primarily DNA synthesis in B16 melanoma cells. *Biochemistry 37*, 5136−5146.

(9) Lisgarten, J. N., Coll, M., Portugal, J., Wright, C. W., and Aymami, J. (2002) The antimalarial and cytotoxic drug cryptolepine intercalates into DNA at cytosine-cytosine sites. *Nat. Struct. Biol. 9*, 57−60.

(10) Guittat, L., Alberti, P., Rosu, F., Van Miert, S., Thetiot, E., Pieters, L., Gabelica, V., De Pauw, E., Ottaviani, A., Riou, J.-F., and Mergny, J.-L. (2003) Interactions of cryptolepine and neocryptolepine with unusual DNA structures. *Biochimie 85*, 535−547.

(11) Guyen, B., Schultes, C. M., Hazel, P., Mann, J., and Neidle, S. (2004) Synthesis and evaluation of analogues of 10*H*-indolo[3,2-*b*]quinoline as G-quadruplex stabilizing ligands and potential inhibitors of the enzyme telomerase. *Org. Biomol. Chem. 2*, 981−988.

(12) Zhou, J.-L., Lu, Y.-J., Ou, T.-M., Zhou, J.-M., Huang, Z.-S., Zhu, X.-F., Du, C.-J., Bu, X.-Z., Ma, L., Gu, L.-Q., Li, Y.-M., and Chan, A. S.-C. (2005) Synthesis and evaluation of quindoline derivatives as G-quadruplex inducing and stabilizing ligands and potential inhibitors of telomerase. *J. Med. Chem. 48*, 7315−7321.

(13) Riechert-Krause, F., Eick, A., Grünert, R., Bednarski, P. J., and Weisz, K. (2011) In vitro anticancer activity and evaluation of DNA duplex binding affinity of phenyl-substituted indoloquinolines. *Bioorg. Med. Chem. Lett. 21*, 2380−2383.

(14) Povsic, T. J., Strobel, S. A., and Dervan, P. B. (1992) Sequence-specific double-strand alkylation, and cleavage of DNA mediated by triple-helix formation. *J. Am. Chem. Soc. 114*, 5934−5941.

(15) Hélène, C., Thuong, N. T., and Harrel-Bellan, A. (1992) Control of gene expression by triple helix-forming oligonucleotides. The antigene strategy. *Ann. N.Y. Acad. Sci. 660*, 27−36.

(16) Ghosh, I., Stains, C. I., Ooi, A. T., and Segal, D. J. (2006) Direct detection of double-stranded DNA: Molecular methods and applications for DNA diagnostics. *Mol. BioSyst. 2*, 1−11.

(17) Eick, A., Xiao, Z., Langer, P., and Weisz, K. (2008) Spectroscopic studies on the formation and thermal stability of DNA triplexes with a benzoannulated *δ*-carboline-oligonucleotide conjugate. *Bioorg. Med. Chem. 16*, 9106−9112.

(18) Eick, A., Riechert-Krause, F., and Weisz, K. (2010) Spectroscopic and calorimetric studies on the triplex formation with oligonucleotide-ligand conjugates. *Bioconjugate Chem. 21*, 1105−1114.

(19) Eick, A., Riechert-Krause, F., and Weisz, K. (2012) Binding and NMR structural studies on indoloquinoline-oligonucleotide conjugates targeting duplex DNA. *Bioconjugate Chem. 23*, 1127−1137.

(20) Jain, A., Wang, G., and Vasquez, K. M. (2008) DNA triple helices: Biological consequences and therapeutic potential. *Biochimie 90*, 1117−1130.

(21) Strekowski, L., Wolinska, E., and Mojzych, M. (2007) DNA triple-helix stabilizing agents. In *Synthetic and Biophysical Studies of DNA Binding Compounds* (Lee, M., and Strekowski, L., Eds.) pp 263−278, Transworld Research Network, Kerala, India.

(22) Arya, D. P. (2011) New approaches toward recognition of nucleic acid triple helices. *Acc. Chem. Res. 44*, 134−146.

(23) Lavrado, J., Cabal, G. G., Prudêncio, M., Mota, M. M., Gut, J., Rosenthal, P. J., Díaz, C., Guedes, R. C., dos Santos, D. J. V. A., Bichenkova, E., Douglas, K. T., Moreira, R., and Paulo, A. (2011) Incorporation of basic side chains into cryptolepine scaffold: Structure−antimalarial activity relationships and mechanistic studies. *J. Med. Chem. 54*, 734−750.

(24) Langer, P., Anders, J. T., Weisz, K., and Jähnchen, J. (2003) Efficient synthesis of 2-alkylidene-3-iminoindoles, indolo[1,2-*b*]-isoquinolin-5-ones, *δ*-carbolines, and indirubines by domino and sequential reactions of functionalized nitriles. *Chem.—Eur. J. 9*, 3951−3964.

(25) Eftink, M. R. (1997) Fluorescence methods for studying equilibrium macromolecule-ligand interactions. *Methods Enzymol. 278*, 221−257.

(26) Rettig, M., Kamal, A., Ramu, R., Mikolajczak, J., and Weisz, K. (2009) Spectroscopic and calorimetric studies on the DNA recognition of pyrrolo[2,1-*c*][1,4]benzodiazepine hybrids. *Bioorg. Med. Chem. 17*, 919−928.

(27) Cheng, Y.-C., and Prusoff, W. H. (1973) Relationship between the inhibition constant (K_I) and the concentration of inhibitor which

causes 50% inhibition (I_{50}) of an enzymatic reaction. *Biochem. Pharmacol. 22*, 3099−3108.
(28) Drake, A. F. (2001) in *Protein-ligand interactions: Structure and spectroscopy* (Harding, S. E., and Chowdhry, B. Z., Eds.) pp 123−168, Oxford University Press, Oxford, U.K.
(29) Völker, J., and Klump, H. H. (1994) Electrostatic effects in DNA triple helices. *Biochemistry 33*, 13502−13508.
(30) Leitner, D., and Weisz, K. (2000) Sequence-dependent stability of intramolecular DNA triple helices. *J. Biomol. Struct. Dyn. 17*, 993−1000.
(31) Keppler, M. D., James, P. L., Neidle, S., Brown, T., and Fox, K. R. (2003) DNA sequence specificity of triplex-binding ligands. *Eur. J. Biochem. 270*, 4982−4992.
(32) Boger, D. L., Fink, B. E., Brunette, S. R., Tse, W. C., and Hedrick, M. P. (2001) A simple, high-resolution method for establishing DNA binding affinity and sequence selectivity. *J. Am. Chem. Soc. 123*, 5878−5891.
(33) Boger, D. L., and Tse, W. C. (2001) Thiazole orange as the fluorescent intercalator in a high resolution FID assay for determining DNA binding affinity and sequence selectivity of small molecules. *Bioorg. Med. Chem. 9*, 2511−2518.
(34) Lubitz, I., Zikich, D., and Kotlyar, A. (2010) Specific high-affinity binding of thiazole orange to triplex and G-quadruplex DNA. *Biochemistry 49*, 3567−3574.
(35) Xue, L., Xi, H., Kumar, S., Gray, D., Davis, E., Hamilton, P., Skriba, M., and Arya, D. P. (2010) Probing the recognition surface of a DNA triplex: Binding studies with intercalator-neomycin conjugates. *Biochemistry 49*, 5540−5552.
(36) Xi, H., Kumar, S., Dosen-Micovic, L., and Arya, D. P. (2010) Calorimetric and spectroscopic studies of aminoglycoside binding to AT-rich DNA triple helices. *Biochimie 92*, 514−529.
(37) Haq, I., Ladbury, J. E., Chowdhry, B. Z., and Jenkins, T. C. (1996) Molecular anchoring of duplex and triplex DNA by disubstituted anthracene-9,10-diones: Calorimetric, UV melting, and competition dialysis studies. *J. Am. Chem. Soc. 118*, 10693−10701.
(38) Arya, D. P., Micovic, L., Charles, I., Coffee, R. L., Jr., Willis, B., and Xue, L. (2003) Neomycin binding to Watson-Hoogsteen (W-H) DNA triplex groove: A model. *J. Am. Chem. Soc. 125*, 3733−3744.
(39) Haq, I., Chowdhry, B. Z., and Jenkins, T. C. (2001) Calorimetric techniques in the study of high-order DNA-drug interactions. *Methods Enzymol. 340*, 109−149.
(40) Ren, J., Jenkins, T. C., and Chaires, J. B. (2000) Energetics of DNA intercalation reactions. *Biochemistry 39*, 8439−8447.
(41) Chaires, J. B. (2006) A thermodynamic signature for drug-DNA binding mode. *Arch. Biochem. Biophys. 453*, 26−31.
(42) Chaires, J. B. (1997) Energetics of drug-DNA interactions. *Biopolymers 44*, 201−215.
(43) Xi, H., Davis, E., Ranjan, N., Xue, L., Hyde-Volpe, D., and Arya, D. P. (2011) Thermodynamics of nucleic acid "shape readout" by an aminosugar. *Biochemistry 50*, 9088−9113.
(44) Wang, G., and Vasquez, K. M. (2004) Naturally occurring H-DNA-forming sequences are mutagenic in mammalian cells. *Proc. Natl. Acad. Sci. U.S.A. 101*, 13448−13453.